HydroResearch 6 (2023) 279–292

Contents lists available at ScienceDirect

HydroResearch

journal homepage: http://www.keaipublishing.com/en/journals/hydroresearch/

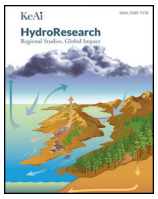

Climate change impact on water availability in the Himalaya: Insights from Sunkoshi River basin, Nepal

Raghu Nath Prajapati [a,*], Nurazim Ibrahim [a], Bhesh Raj Thapa [b]

[a] Infrastructure University Kuala Lumpur (IUKL), Malaysia
[b] Universal Engineering and Science College, Nepal

ARTICLE INFO

Article history:
Received 15 July 2023
Received in revised form 6 October 2023
Accepted 7 October 2023
Available online 10 October 2023

Keywords:
Climate change impact
Global climate model (GCM)
Shared socioeconomic pathway (SSP)
SWAT
Sunkoshi River basin

ABSTRACT

Changing streamflow is one of the most visible consequences of climate change. In this study, the Soil and Water Assessment Tool (SWAT) model was used to investigate the significant effects of climate change on streamflow in a Himalayan River. We incorporated information from several Global Climate Models (GCM), considering two climate scenarios: SSP 2.45 and SSP 5.85, which are part of Shared Socioeconomic Pathways (SSPs) for the future periods of 2022–2030 and 2031–2050. Substantial patterns in temperature and rainfall changes were identified using ensemble modeling. Under both SSPs 2.45 and 5.85, the results indicated a rising trend in temperatures from January to June, a decline from June to September, and a marginal increase from October to December. Additionally, annual rainfall, real evapotranspiration, and river flow are anticipated to rise by 17.67–21.79%, up to 0.93%, and 23–53%, respectively in the upper region of the study basin. Conversely, across the two future periods and scenarios, the lower region is depicted to have a decline in rainfall of 20.84–36.34%, evapotranspiration of up to 4.35%, and river flow of 38–65%. These findings will be invaluable for the design and construction of climate-resilient water resources related projects in the Himalayan regions, such as Nepal.

1. Introduction

The timing, intensity, pattern, temperature, and discharge of rainfall are all influenced by climate change, which ultimately impacts on hydrological cycle both locally and worldwide. As per the Intergovernmental Panel on Climate Change 6th Assessment Report (IPCC, 2023), there was a 0.85 °C rise in global temperature between 1881 and 2012 (Stocker et al., 2013). Numerous studies have repeatedly shown a perceivable rise in temperatures in the Himalayan regions (Bharati et al., 2019). As a consequence, the supply of water in rivers, especially in fall and spring, is expected to be adversely affected by the temperature rise (Maskey et al., 2011). By 2100, researchers expect Nepal's average temperature to climb by 5.80 °C, with higher elevations observing more significant warming (Mishra et al., 2021). In addition, the study highlights that the capacity to store water in atmosphere will increase by 7% for every 1^0C increase in temperature (Trenberth, 2011), leading to more frequent and heavy rainstorm events that will alter basin-scale stream flow patterns. One of the mathematical models used to simulate the general circulation of the planetary atmosphere is the global climate model (GCM). The model's limited geographic resolution makes it unsuitable for local hydrological models, but it is valuable for analyzing and forecasting long-term climatic patterns (Marchi et al., 2020). Both GCMs and regional climate models (RCMs) can provide forecasts of future climate conditions. When considering local-scale basins, RCMs are preferred due to their superior spatial resolution, offering more accurate simulations for smaller regions (Miyamoto et al., 2013; Navarro-Racines et al., 2020; Satoh et al., 2019) compared to GCMs. To assess the effects of climate change on a local scale, RCM forecasts must first be adjusted for biases resulting from the coarse spatial resolution of the model. Researchers have developed downscaling methods, such as statistical techniques like empirical quantile mapping (QM) (Maraun, 2013), which are employed to correct these biases (Pandey et al., 2020a; Shrestha et al., 2017). These techniques make use of Regional Climate Models (RCMs). Representative Concentration Pathways (RCPs) and Shared Socioeconomic Pathways (SSPs) are two climate change scenarios created by the Coupled Model Intercomparison Project Phase (CMIP) to examine potential futures for the planet under various climate change mitigation levels (Sato et al., 2007; Xu and Yang, 2015). The IPCC has developed these scenarios for the latest phase of the Coupled Model Intercomparison Project, known as CMIP6 (Xu et al., 2021). These scenarios, including Representative Concentration Pathways (RCPs) and Shared Socioeconomic Pathways (SSPs), play vital roles in climate modeling (Basheer et al., 2016). However, SSPs

* Corresponding author.
E-mail address: 082101900006@s.iukl.edu.my (R.N. Prajapati).

https://doi.org/10.1016/j.hydres.2023.10.002

go beyond greenhouse gas emissions by considering socioeconomic aspects, while RCPs primarily focus on greenhouse gas concentrations and emission pathways (Imada et al., 2019; Prein et al., 2017).

SSPs provide a more comprehensive understanding of how various societal decisions and behaviors can influence future climate outcomes (Adachi and Tomita, 2020). Climate models utilize five distinct SSP scenarios to explore how socioeconomic factors, such as population growth and economic development, might impact greenhouse gas emissions in the future. These SSPs are designed to complement the RCPs, offering a more holistic perspective on how various factors can interact to shape future climate outcomes. Temperature and precipitation data from Global Climate Models (GCMs) are utilized in hydrological models such as the Soil and Water Assessment Tools (SWAT) to project future hydrological trends (Tan et al., 2014). Several factors, including spatial dimensions, adaptability, and calibration simplicity, must be considered when selecting an appropriate hydrological model.

The semi-distributed hydrological model SWAT can simulate the potential impacts of climate change on various watersheds. Worldwide, SWAT has been extensively employed to assess the effects of climate change in multiple river basins, such as the Koshi River Basin in Nepal (Agarwal et al., 2015), the Kelantan River Basin in Malaysia (Tan et al., 2017), and numerous countries (Faramarzi et al., 2017; Schuol et al., 2008), including India, where it has been used to quantify climate change impacts in twelve major rivers (Gosain et al., 2006).

In Nepal, the use of SWAT has played a crucial role in evaluating future projections and the effects of climate change in various watershed studies, including Babai (Mishra et al., 2021), Karnali (Dahal et al., 2020; Pandey et al., 2020a), Chamelia (Pandey et al., 2019), Kaligandaki (Bajracharya et al., 2018), Indravati (Palazzoli et al., 2015), West Seti (Gurung et al., 2013), and the Bagmati (Dahal et al., 2016; Gurung et al., 2013).

While SWAT provides valuable insights, it is important to note that its forecasts are based on assumptions and approximations, and their accuracy is directly linked to the quality of the input data. Therefore, caution should be exercised when interpreting their projections, and a diverse range of information sources should be considered when making decisions related to agriculture and water resources.

The aim of the current study was to evaluate temperature and rainfall anomalies in the Himalayan region, with a specific focus on recent and upcoming decades. Additionally, this research sought to investigate the potential influence of climate change on hydrological variations in 2030 and 2050 using the SWAT hydrological tool, establishing a connection between present and future climatic shifts and assessing associated risks.

The study had the following objectives: (i) Assess the uncertainty in SWAT model performance by varying the number of sub-basins, HRUs, and elevation bands, (ii) Project basin climate by employing the Statistical Downscaling Method (SDM) bias correction method, (iii) Examine the impacts of climate change on streamflow under the SSP 2.45 and SSP 5.85 scenarios. The findings of this study should prove valuable not only for the development of water management plans in the SRB but also for other river basins sharing similar geographical and climatic characteristics.

2. Study area

In the central and northern regions of Nepal and Tibet, lies the Sunkoshi River Basin (SRB), covering an area of approximately 5000 km^2, with roughly 40% of its catchment situated in Tibet, China. This basin encompasses the Sunkoshi River, a significant tributary of the Koshi River. As illustrated in Fig. 1, the SRB is situated between latitudes 27° 31′ 36“ and 28° 30’ 35” north and longitudes 85° 25′ 53“ to

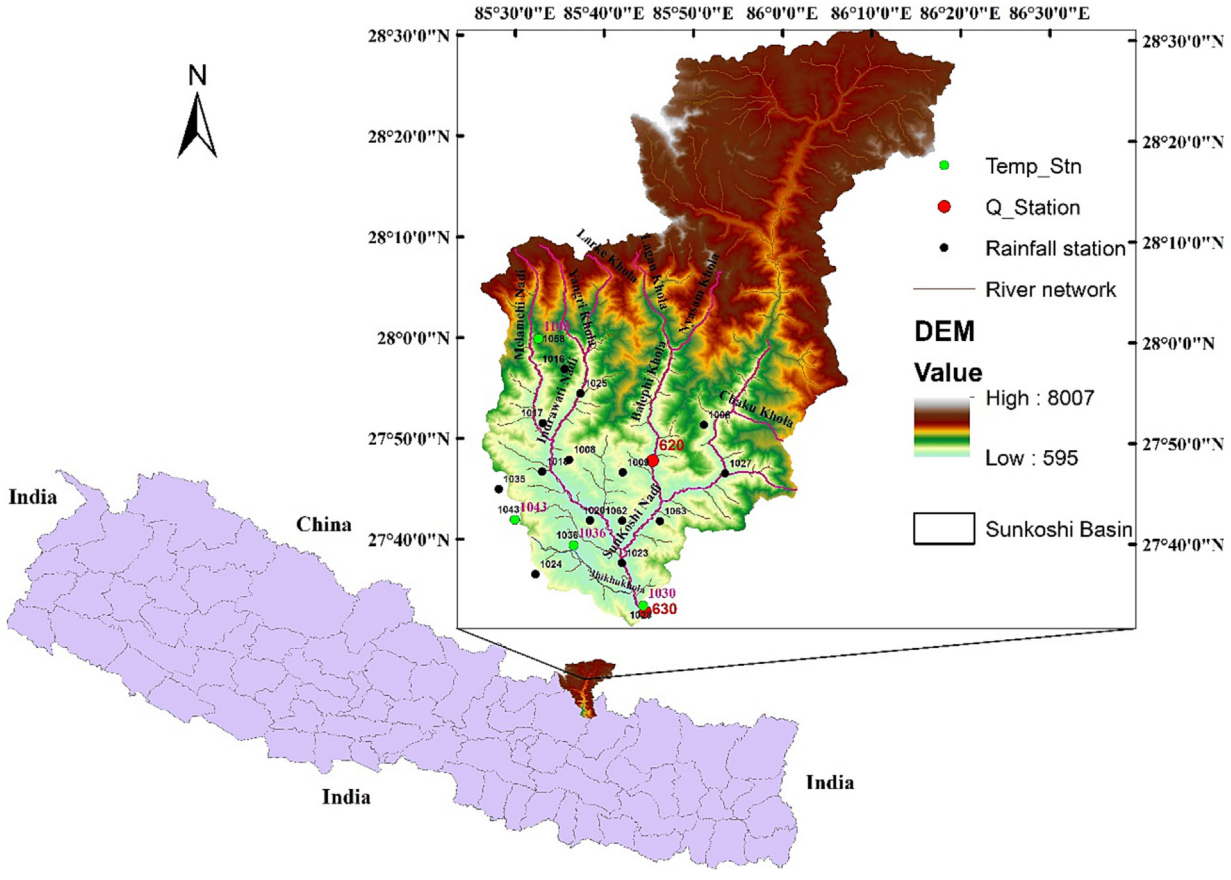

Fig. 1. Location, DEM (Digital Elevation Model), Rainfall stations, Q (hydrological) stations, Temperature stations and River Tributaries of the SRB.

86° 19' 53" east. Among its major tributaries are the Bhotekosh, Melamchi, Indrawati, Belephi, and Jhikhkhukhola rivers. The SRB's length, as determined by the Pachuwar Ghat Stream Gauge Station (630), is approximately 148.4 km. Elevations within the basin vary from 546 m to over 5000 m above mean sea level (AMSL). The Sunkoshi River Basin (SRB) serves as a critical water source for hydropower, agriculture, and various other purposes in Nepal and India. Despite its significance, limited research has been conducted to comprehensively understand its hydrology, water sources, and the potential impacts of climate change on the region (Pandey et al., 2020b; Rocheta et al., 2017).

Figure 2a illustrates the land use categorization of the SRB, revealing that approximately 12% of the basin's area is designated for agricultural use, while roughly 37% is covered by forests. Fig. 2b provides insights into the three main soil types in the region, which are Cambisol, Regosol, and Luvisol. In underdeveloped nations like Nepal, it is common to have a limited density of climatological stations. Climatological and hydrological stations were not given priority in the SRB due to its challenging geographical terrain, often characterized by higher altitudes (Mishra et al., 2018). Consequently, existing stations are predominantly situated at lower elevations. Data collected by the Department of Hydrology and Meteorology (DHM) in Nepal, spanning from 1980 to 2015 and obtained from 16 rain gauge stations (as depicted in Fig. 1), reveal that the average annual minimum and maximum precipitation amounts to 494 mm and 3363 mm, respectively. The monsoon season, occurring from June to September, contributes to approximately 80% of the annual rainfall. According to statistics gathered from four stations (1030, 1036, 1043, and 1103) over the same period, the average maximum temperature (Tmax) and minimum temperature (Tmin) in the region are recorded at 28 °C and 8 °C, respectively.

3. Materials and methods

This study employs a model-based approach to assess the distribution of water availability within the SRB. Fig. 3 provides an overview of the research methodology. Future climate conditions were projected using various climate scenarios, including SSP 2.45 and SSP 5.85. The assessment of water availability in both the present and future relied on a hydrological model developed with SWAT.

3.1. Data collection

Meteorological and hydrological data were provided by the Department of Hydrology and Meteorology (DHM) in Nepal. Rainfall data spanning from 1980 to 2015 were collected from 16 locations, as depicted in Fig. 1. However, data on maximum and minimum temperatures were available only from four climatically stations (1030, 1036, 1043, and 1103). For calibration and validation, data from the Jalire (620) and Pachuwar Ghat (630) hydrological stations were used in this study. The entire SRB lacked data on humidity, daylight hours, and wind speed. All hydrological and meteorological data were collected on a daily basis. Additionally, the study incorporated Digital Elevation Model (DEM), soil, and land use data as inputs for the SWAT model, alongside climatic data. The study sourced soil type maps from https://data.isric.org, a 30-m resolution land use map from https://livingatlas.arcgis, and a 30-m resolution DEM from http://srtm.csi.

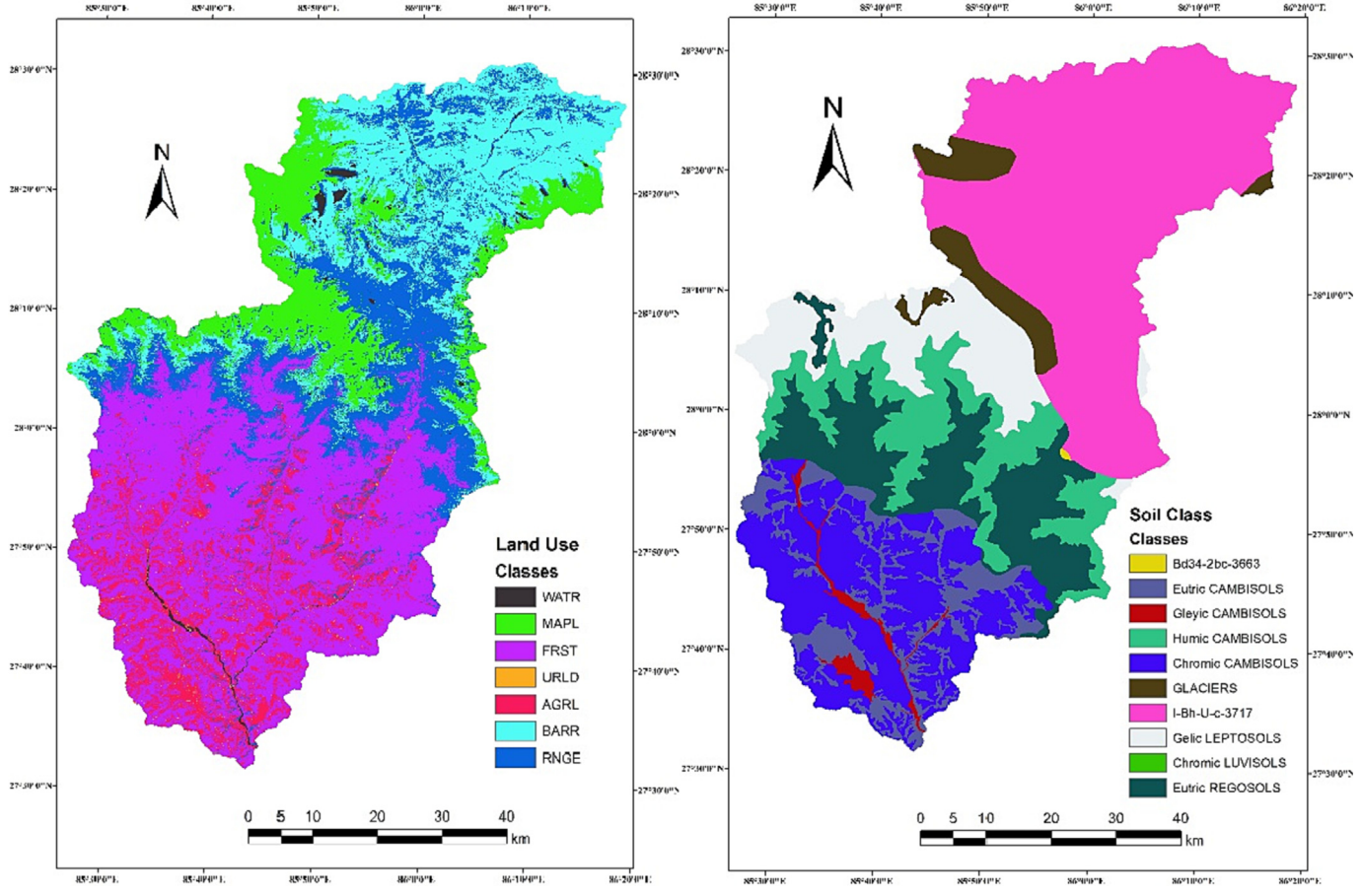

Fig. 2. Classification of a) Land Use and b) Soil Type in Sunkoshi River Basin.

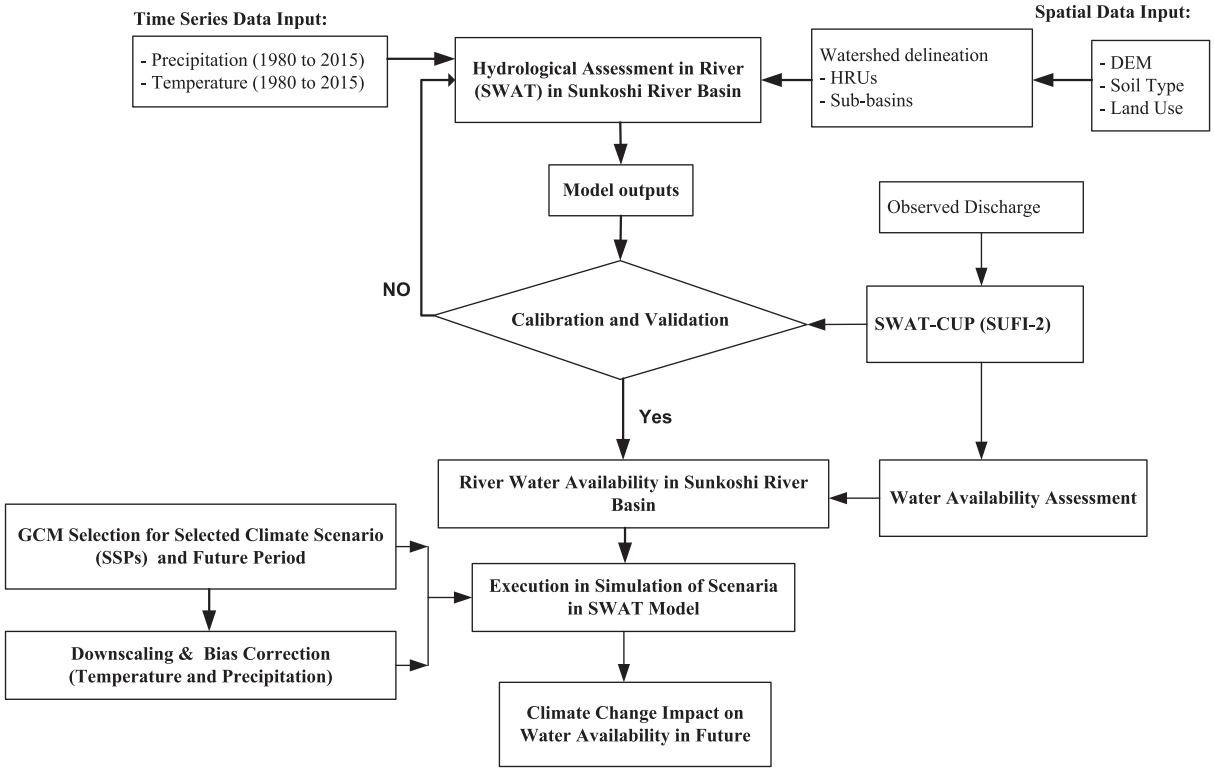

Fig. 3. A methodological framework to evaluate climate change effects in SRB using SWAT Model. DEM stands for Digital Elevation Model, SUFI is a sequential uncertainty-fitting technique and HRU is Hydrological Response Unit.

cgiar.org/srtmdata (Uddin et al., 2015). These datasets were instrumental in enhancing the analysis and modeling of the SRB.

3.2. Shared socioeconomic pathways scenario

Shared Socioeconomic Pathways (SSPs) encompass a set of scenarios designed to depict potential future shifts in human civilization. These transformations could be driven by factors such as population growth, economic advancements, technological innovations, and more. SSPs hold critical importance in projecting future greenhouse gas emissions and their consequent impacts on climate change. They classify the Earth's energy budget imbalance caused by fluctuations in greenhouse gas concentrations in the atmosphere into five distinct levels of radiative forcing. Within the spectrum of SSPs, each level signifies a specific trajectory. For instance, SSP1–1.9 envisions that by the year 2100, global warming can be limited to an increase of less than 1.5 °C compared to pre-industrial levels, with radiative forcing peaking at 1.9 W/m^2 before declining. In contrast, SSP5–8.5 suggests excessive greenhouse gas emissions and inadequate climate mitigation, resulting in global warming of 4–6 °C above pre-industrial levels by the century's end, with a peak radiative forcing of 8.5 W/m^2 before a subsequent decrease (Richter and Tokinaga, 2020). For this study, the scenarios employed were SSP 2.45 and SSP 5.85. In the initial stages of the research, Global Climate Models (GCMs) were selected based on a comprehensive literature review. Four widely utilized GCMs with complete data availability for SSPs in comparable regions of Nepal were utilized (Almazroui et al., 2020; Pandey et al., 2020a). Subsequently, downscaled data derived from these GCMs were compared with meteorological data from the baseline period spanning from 1980 to 2014. The Model for Interdisciplinary Research on Climate Version 6 (MIROC6) was collaboratively developed by the Japan Agency for Marine-Earth Science and its associated institutions. The Norwegian Earth System Model, created by the Norwegian Climate Centre, is referred to as NorESM. The global climate model known as MPI-ESM1–2-LR, or Max Planck Institute Earth System Model version 1.2, Low Resolution, was developed by the Max Planck Institute for Meteorology in Germany. These models are all part of the Coupled Model Intercomparison Project Phase 6 (CMIP6). Following a comparison of their results with observable data using bias adjustment techniques, the GCM that best suited the research region was chosen. This GCM is well-suited to the study area and has a history of extensive use in climate forecasting.

3.3. Bias correction

Given the inherent limitations of climate change models, bias adjustment becomes imperative when applied at the local level. These models, operating at coarse scales, often fall short in effectively capturing local climatic variations, resulting in systematic inaccuracies or biases. Aligning model outputs with observed local climate data through bias correction enhances model accuracy, a crucial aspect for informed decision-making. However, the application of this technique requires caution to avoid introducing new errors. While bias correction improves the precision of local climate model estimates, it cannot completely eliminate all sources of uncertainty. Downscaling methods are employed to address the coarse spatial resolution data from Global Climate Models (GCMs) (GIORGI and GAO, 2018). There are two primary downscaling approaches: statistical and dynamic downscaling. Statistical Downscaling Method (SDM) establishes an empirical link between GCM outputs and ground data from specific stations, while dynamic downscaling integrates a Regional Climate Model (RCM) into the GCM (Teutschbein and Seibert, 2012; Wang et al., 2004). In this study, biases in temperature and precipitation simulations produced by climate models are adjusted using a statistical downscaling technique known as quantile mapping (QMAP) bias downscaling, implemented in R with the qmap package (Colette et al., 2012; Xu and Yang, 2015). QMAP bias downscaling is a widely adopted method in climate research to enhance the accuracy of climate model predictions for temperature and precipitation (Dai et al., 2020). When estimating future climates, the QMAP technique assumes

that the bias in historical data remains constant. QMAP achieves this by establishing appropriate transfer functions to align quantiles of RCM data with observed data (Shrestha et al., 2017). Performance assessment of climate models includes metrics such as mean, standard deviation (SD), as well as R^2, and root mean square error (RMSE).

3.4. Model setup, calibration, and validation

Through the precise adjustment of projected climate data, SWAT proves to be a valuable tool for exploring future climate changes (Agarwal et al., 2015). The basin is divided into multiple sub-basins and Hydrological Response Units (HRUs) based on land use, slope, and soil characteristics. In this study, the SRB model was constructed using ArcSWAT 2012, integrated into the ArcGIS 10.4 program. SWAT simulates hydrological factors and runoff outcomes at the HRU level, which are then aggregated at the catchment scale using a weighted average of HRU results (Abbaspour et al., 2019). The research revealed that relying solely on land use, soil, and slope parameters to delineate HRUs within a sub-basin is insufficient for capturing the nuanced sub-basin characteristics. To address this, various scenarios were explored by adjusting the threshold combinations of land use, soil, and slope. A 10% criterion for each component resulted in a more accurate representation of streamflow when combined, yielding a total of 805 HRUs for the entire SRB. This approach led to a more comprehensive and inclusive database, providing a more realistic portrayal of the region's diversity and variability (Kumar and Bhattacharjya, 2020).

Utilizing the provided rainfall and temperature data as inputs to the model, the Hargreaves potential evapotranspiration (PET) technique was employed for PET calculations. Following a five-year warm-up phase spanning from 1980 to 1985, the SWAT model was executed from 1985 to 2015. SWAT-CUP is a freely available software application designed for the automatic calibration of SWAT models. It offers various calibration methods, including MCMC (Markov Chain Monte Carlo), PSO (Particle Swarm Optimization), GLUE (Generalized Likelihood Uncertainty Estimation), and SUFI-2 (Sequential Uncertainty Fitting 2). The SUFI-2 technique is particularly advantageous in terms of computational efficiency and model performance when calibrating and assessing uncertainties in a model (Pang et al., 2020; Singh and Saravanan, 2020). In this study, the SUFI-2 tool within SWAT-CUP was employed for model calibration. A total of 17 parameters were used to achieve the best fit, with at least 100 simulations conducted. Calibration involves adjusting model components to establish a strong correlation between model outputs and observed data. The model was both calibrated and validated for monthly and daily applications at two key locations within the study area: the primary outlet at the Pachuwar Ghat station (630) and a hydrological station situated in the middle of the study area, known as Jalire (620), as indicated in Fig. 1. During validation, input parameter values of the model remain unaltered. In this study, the calibration was performed using a heuristic approach, which involves estimating the number of simulations required for each parameter based on the total number of parameters engaged in the calibration process. Several metrics, including R^2, Nash-Sutcliffe Efficiency (NSE), and Percent Bias (PBIAS), were employed to evaluate the model's performance. Moriasi et al. (2007) suggest that a PBIAS within 25%, NSE greater than 0.5, and R^2 exceeding 0.6 serve as indicators of satisfactory model performance. In the context of this study, the results demonstrate a commendable level of model performance, with R^2 and NSE values surpassing 0.8 and 0.7 for both monthly and daily calibration and validation at the outlet stations.

4. Results and discussions

4.1. Performance of bias correction

Bias adjustments were applied to historical simulations spanning from 1985 to 2014, as well as to two future scenarios, namely SSP 2.45 and SSP 5.85, covering the period from 2015 to 2050. During the baseline period, the bias-corrected results closely aligned with the mean monthly values of Tmax, Tmin, and precipitation. These outcomes, depicted in Fig. 4, underscore the remarkable improvement achieved in GCM data quality, with a close match to observed data for Tmin increase and Tmax decrease. Likewise, Fig. 5 presents the achieved results for select rainfall stations, demonstrating that bias-adjusted rainfall closely approximates observed data. The study's findings establish that downscaled data from various models, particularly MIROC6, can be relied upon to provide accurate predictions regarding future water availability in the SRB.

4.2. Model calibration and validation

Figure 6 shows the outcomes daily hydrograph of both calibration and validation. Due to the absence of observed data for certain days within the regular daily time frame, we conducted the calibration and validation processes based on the availability of complete data for both daily and monthly periods. That's why, the different time frame daily and monthly data were used for calibration and validation. This approach ensured that the model's performance was assessed across various time intervals and justified its reliability under different time conditions. In this study, validation covers the years 2007 to 2012, whereas calibration covers the years 1989 to 2007 at the main outlet hydrological station (630) of the study area. Similarly, Fig. 6b illustrates the hydrograph for calibration and validation at the Jalire hydrological station (620), located in the central region of the study area. For calibration, daily flow data from 1990 to 2004 were utilized, while validation tests employed data from 2005 to 2010, with a five-year warm-up phase between 1980 and 1985. The validation process employed the same input parameters as the calibration process. The evaluation was conducted using daily datasets from the outflow hydrological stations (630) and the hydrological stations (620) within the basin. Deterministic parameters, such as NSE and R-squared (R^2), which assess the model's performance, are detailed in Table 1. Although calibration and validation were performed for both hydrological stations at both daily and monthly timescales, Fig. 6 displays only the daily hydrographs. The NSE and R^2 values for calibration at station 630 were 0.73/0.79 (daily) and 0.82/0.91 (monthly), while those for validation were 0.75/0.82 (daily) and 0.84/0.91 (monthly). For the Jalire station (620), the calibration parameters, i.e., NSE and R^2, were 0.74/0.75 for daily and 0.80/0.81 for monthly. Similarly, the validation parameters for daily/monthly were 0.76/0.76 (NSE) and 0.70/0.79 (R^2). The analysis of model evaluation indicates that the model performed admirably. It accurately predicted peak flows during monthly calibration, suggesting its suitability for assessing streamflow volume. However, it may not be suitable for flood estimation and forecasting (Mishra et al., 2018).

4.3. Future temperature

Four distinct models MIROC6, MPI-ESM1–2-LR, NorESM, and CNRM-CM6 were used in the ArcSWAT model to generate the future daily data for maximum and lowest temperatures as well as precipitation. These datasets were modified after bias correction to account for any errors.

The results obtained using the MIROC6 model demonstrated the highest accuracy in predicting future temperatures, while the NorESM model exhibited superior performance in forecasting future flow patterns. Fig. 7 specifically presents a comparison of anticipated monthly average maximum temperatures for SSP 2.45 and SSP 5.85, contrasted with historical averages for the period spanning 1985 to 2014, as simulated by the MIROC6 model. When compared to observed data, the projected Tmax (maximum temperature) and Tmin (minimum temperature) for the near future (2022 to 2030) and mid-future (2031 to 2050) indicated an increase from January to June, followed by a decrease during the monsoon period (June to September). Conversely,

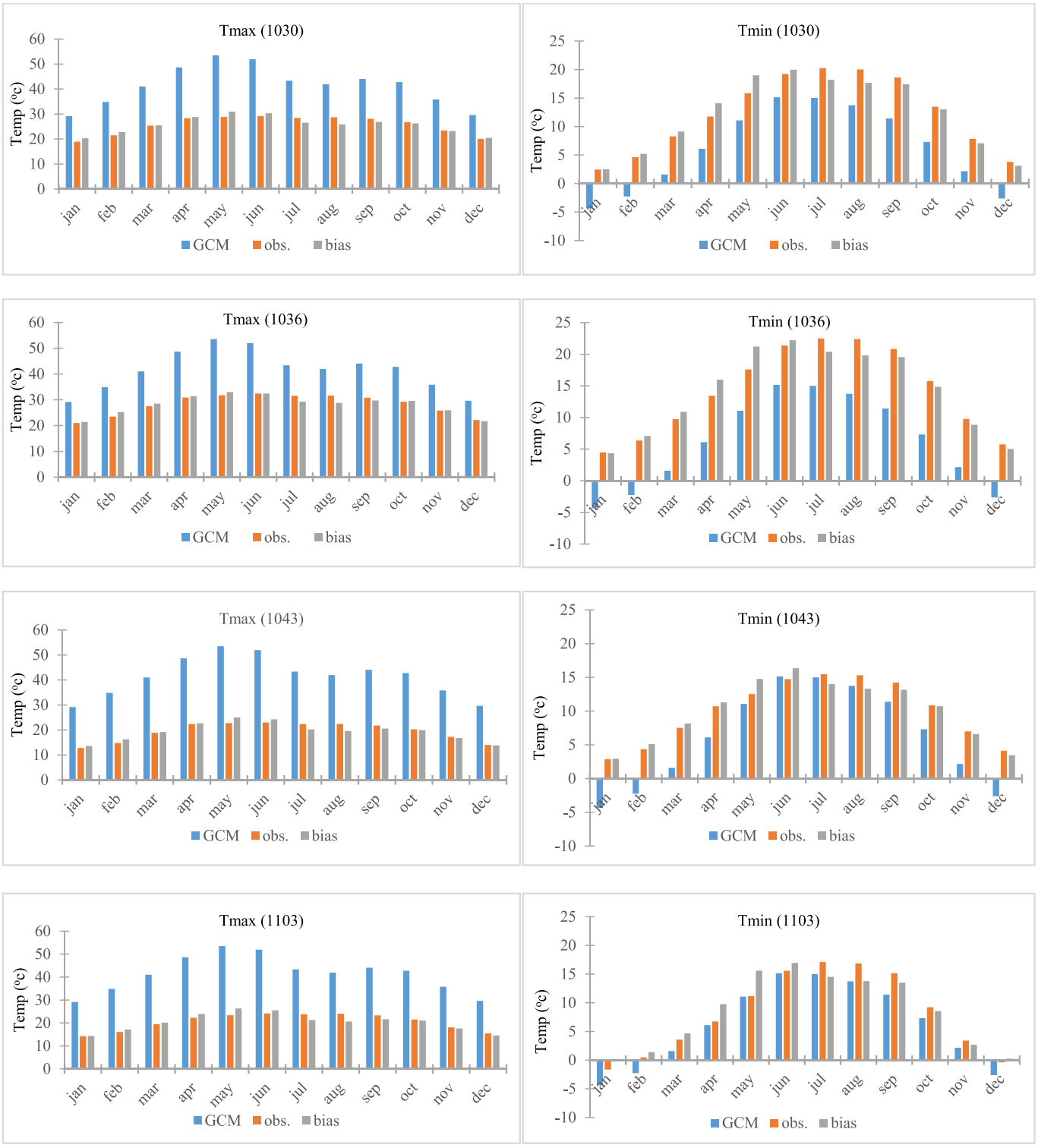

Fig. 4. Mean monthly T_{max} and T_{min} raw GCM, Observed (obs.) and bias-adjusted (bias) temperature at stations 1030, 1036, 1043 and 1103 in the MIROC6 model.

temperatures showed relatively little variation from October to December. These temperature trends were consistent across all four temperature-measuring stations in the SRB. Depending on the specific scenario, temperature increases ranged from 1.62 °C to 5.72 °C, with potential declines of up to 2.91 °C. Tmax was predicted to rise by 0.85 °C to 4.59 °C but could also be projected to decrease by as much as 3.81 °C during the monsoon season.

The downscaled results, as illustrated in Fig. 8 and derived from two global climate models (GCMs), indicated that the average Tmax (maximum temperature) and Tmin (minimum temperature) between 2022 and 2050 would deviate from the average monthly observed Tmax. Specifically, Tmax was projected to increase, while Tmin exhibited variations relative to the baseline period. Notably, Tmin was expected to be higher in the future, except during the monsoon season (June to September). Furthermore, when compared to the SSP 5.85 scenario, all models projected a more rapid rate of temperature increase under the SSP 2.45 scenario. Consequently, these findings demonstrated consistent temperature increase patterns across all GCMs. Additionally,

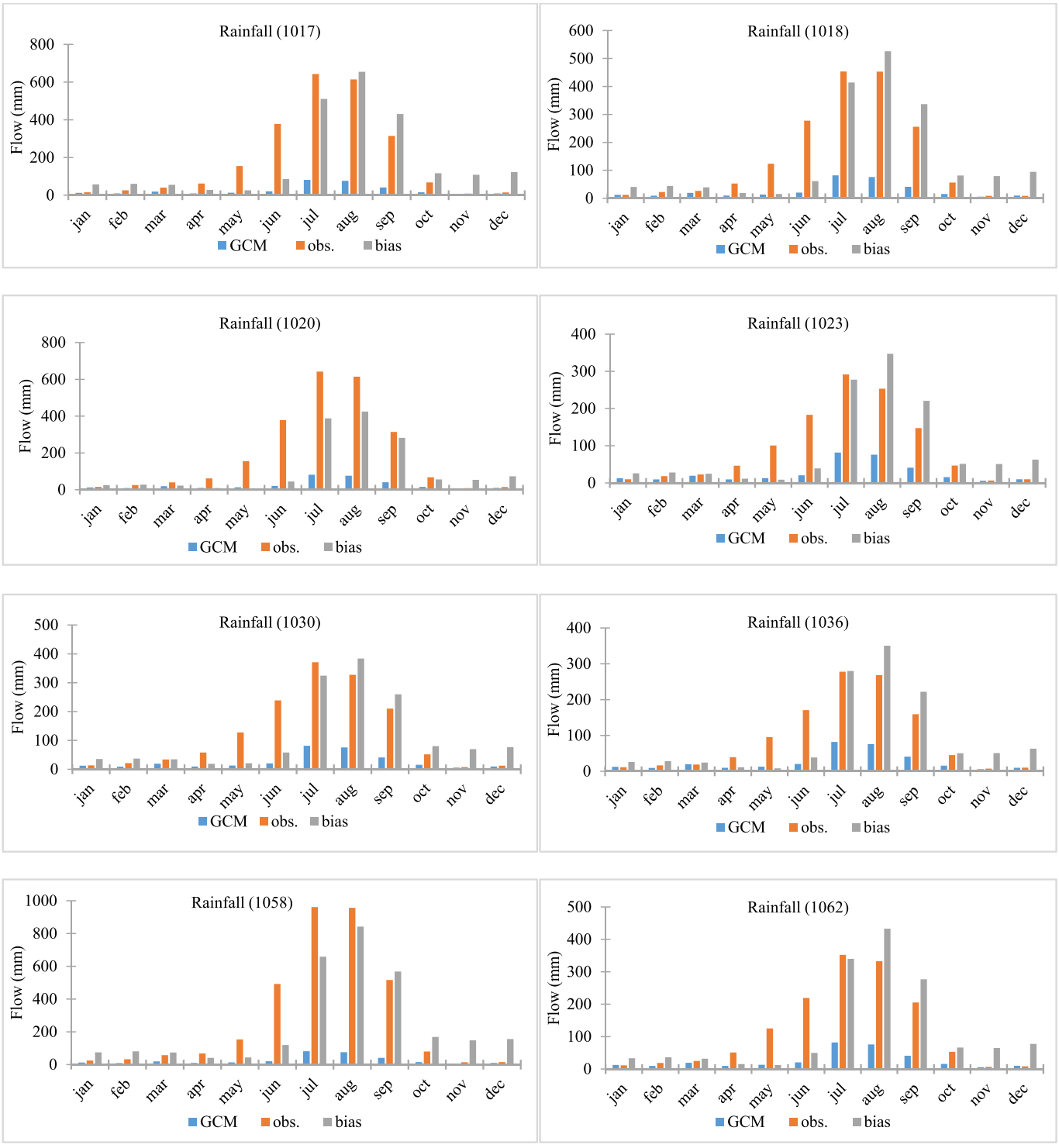

Fig. 5. Mean monthly raw GCM, observed (obs.) and bias-adjusted (bias) rainfall at stations 1017, 1018, 1020, 1023, 1030, 1036, 1058 and 1062 in MIROC6 model.

Fig. 9a depicted a hydrograph indicating a rising trend with a positive slope of 0.018 in the mean annual average temperature over time. This suggests that both average monthly and annual temperatures are anticipated to increase within the study area.

4.4. Future rainfall and streamflow

The average annual precipitation displayed different patterns under the two scenarios. Under the SSP 2.45 scenario, precipitation steadily increased over time, with a positive slope of 0.0051 mm/year, as indicated by the Thiel-Sen slope estimator study (Fig. 9b). Conversely, the SSP 5.85 scenario showed a different trend, with a negative slope of −0.0026 mm/year (Fig. 9c), suggesting a minor decrease in precipitation. Thus, the findings indicated a declining trend in rainfall for the study area.

Table 2 presents estimates of variations in yearly rainfall and flow under the SSP 2.45 and SSP 5.85 scenarios for two future periods. The forecasts indicate that, under the SSP 2.45 scenario, yearly rainfall is

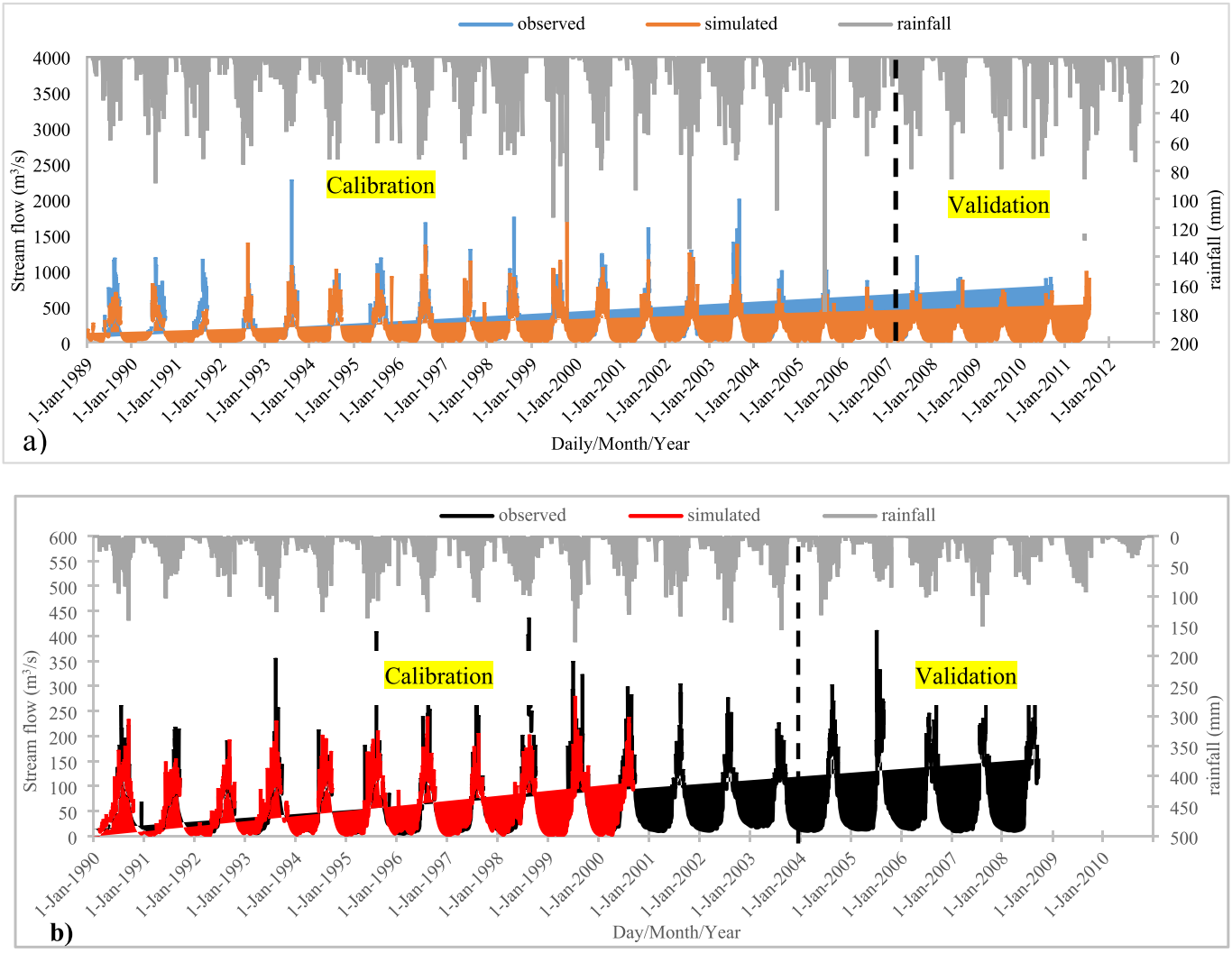

Fig. 6. Hydrograph result of calibration and validation in observed and simulated flow at a daily timescale with rainfall at a) Pachuwar Ghat Station (630) and b) Jalire Station (620).

anticipated to rise by 0.05% in the near future (2022−2030) and by 1.54% in the mid-future (2030–2050) compared to the average baseline period. Conversely, under the SSP 5.85 scenario, the near future is projected to see a 0.11% increase, while the mid-future is expected to experience a 0.01% decline. Flow predictions differ significantly between the two scenarios. The SSP 2.45 scenario predicts a flow decrease of 15.35% in the near future and a 9.27% decrease in the mid-future. In contrast, the SSP 5.85 scenario forecasts a more substantial flow reduction, with a 24.93% decrease in the near future and a 14.37% decrease in the mid-future. Additionally, Fig. 10 displays monthly average rainfall and flow datasets for both observed and anticipated data for the upcoming time periods. Under both SSP scenarios, rainfall and flow exhibit declining trends, with shifts in the monsoon pattern.

Table 2 and Figs. 10b present the streamflow data obtained from the calibrated SWAT model, which utilized expected values for temperature and rainfall based on various climate change scenarios. To assess these results, a comparison was made with the actual streamflow data recorded during the baseline period from 1980 to 2015. Table 2 illustrates a decrease in discharge, indicating a gradual reduction in rainfall over the two future time periods, while temperature shows an increasing trend. Consequently, it can be observed that the yearly streamflow fluctuations do not align consistently with the patterns in rainfall and temperature, as depicted in Fig. 10a and b.

Table 1
Performance characteristics for daily and monthly calibration and validation at hydrological Stations.

Parameters	Calibration		Validation	
Station 630	Daily	Monthly	Daily	Monthly
NSE	0.73	0.82	0.75	0.84
R^2	0.79	0.91	0.82	0.91
Station 620	Daily	Monthly	Daily	Monthly
NSE	0.74	0.80	0.76	0.76
R^2	0.75	0.81	0.70	0.79

4.5. Future water availability

Referring to Fig. 11a, it is observed that the western part of the study area experiences higher rainfall, while the northern part, near the Himalayan region, receives lower rainfall compared to other parts of the study area. Based on the baseline period, there is a declining trend in rainfall magnitude across the entire study area. Furthermore, the findings suggest that the decline in rainfall would be more pronounced under the SSP 5.85 scenario compared to the SSP 2.45 scenario. Similarly, Fig. 11b presents the results related to Potential Evapotranspiration (PET). In the SSP 2.45 scenario, PET is projected to increase, while

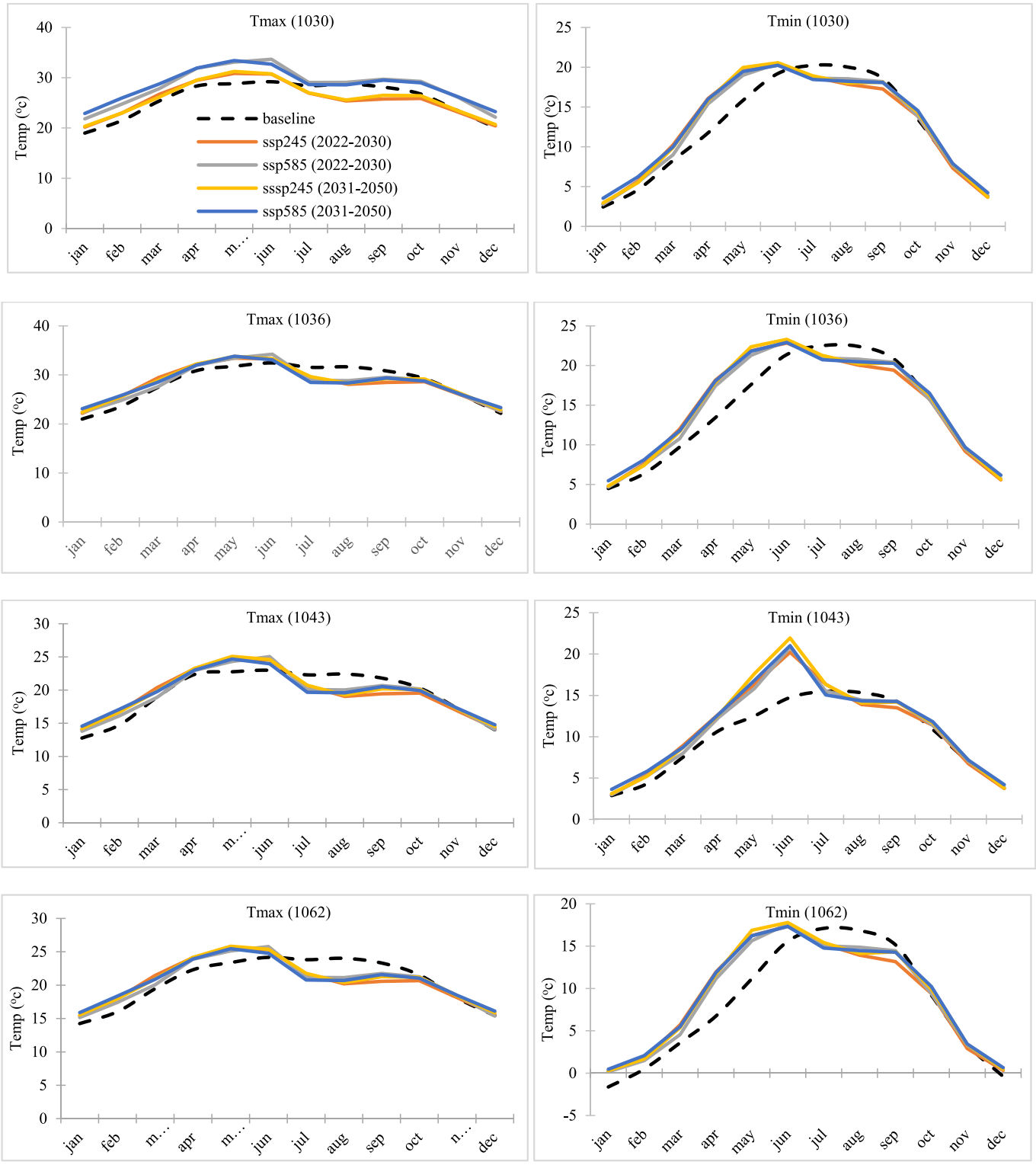

Fig. 7. Comparison of average monthly Tmax and Tmin between observed (1985–2014) and projected in two future periods in two climate scenarios.

in the SSP 5.85 scenario, PET exhibits a decreasing trend in the future. Notably, PET is expected to slightly decrease in the near future (NF) but significantly decrease in the mid-future (MF) under the SSP 5.85 scenario. Regarding climatic changes, both the upper and lower parts of the study area show increases in PET by approximately 0.93% and decreases in PET by −4.35%, respectively. This pattern is mirrored in the river flow, which also exhibits a declining trend. The impact of flow decrease is more pronounced under the SSP 5.85 scenario compared to the SSP 2.45 scenario. Future increases in PET and decreases in flow could be attributed to variations in land use, particularly in agricultural and forested zones such as those in the Indrawati and Melamchi River Tributaries (western part of the sub-basin). Conversely, the arid and Himalayan areas contribute to the observed rise in rainfall and river flow in the higher region. In contrast, the lower and middle portions of the study area are characterized by forests and agricultural lands with chromic CAMBISOLS and humic CAMBISOLS soil, leading to an

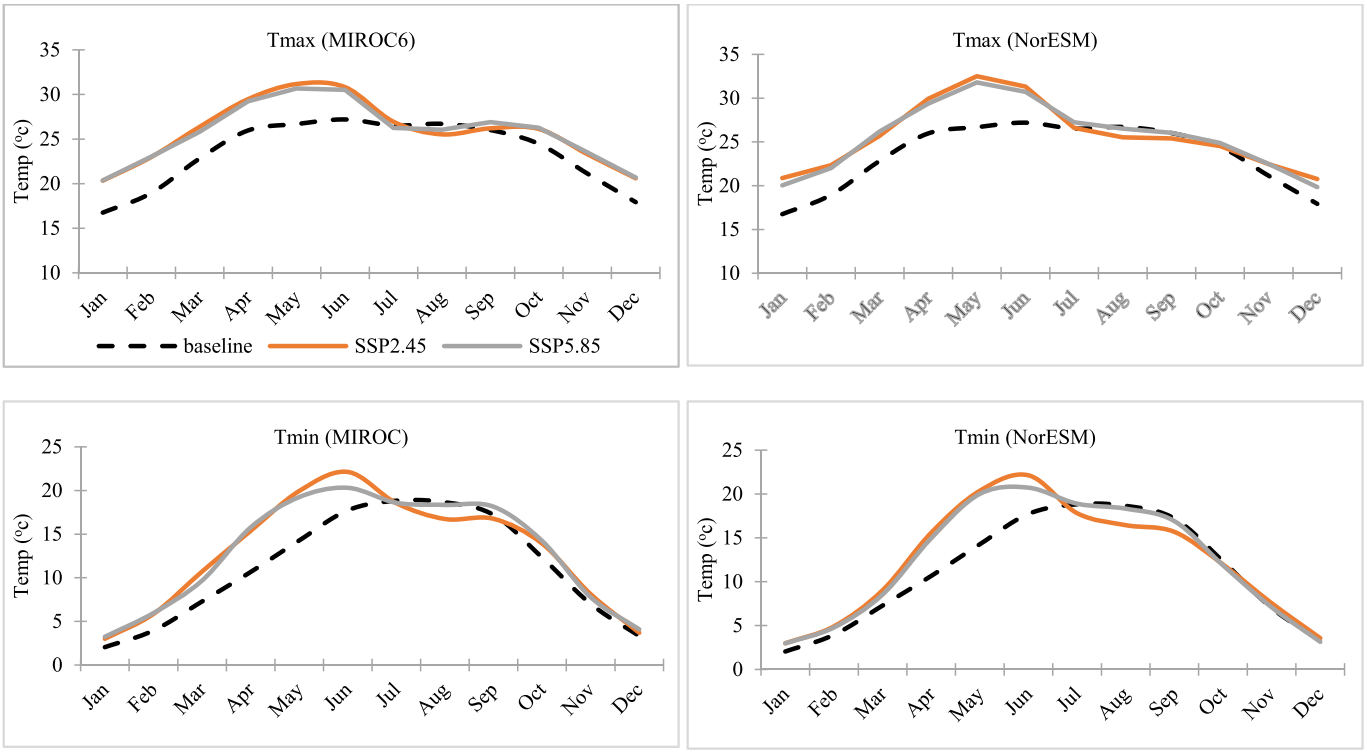

Fig. 8. Average future monthly maximum and minimum temperature generated by MIRIC6 and NorESM climate model.

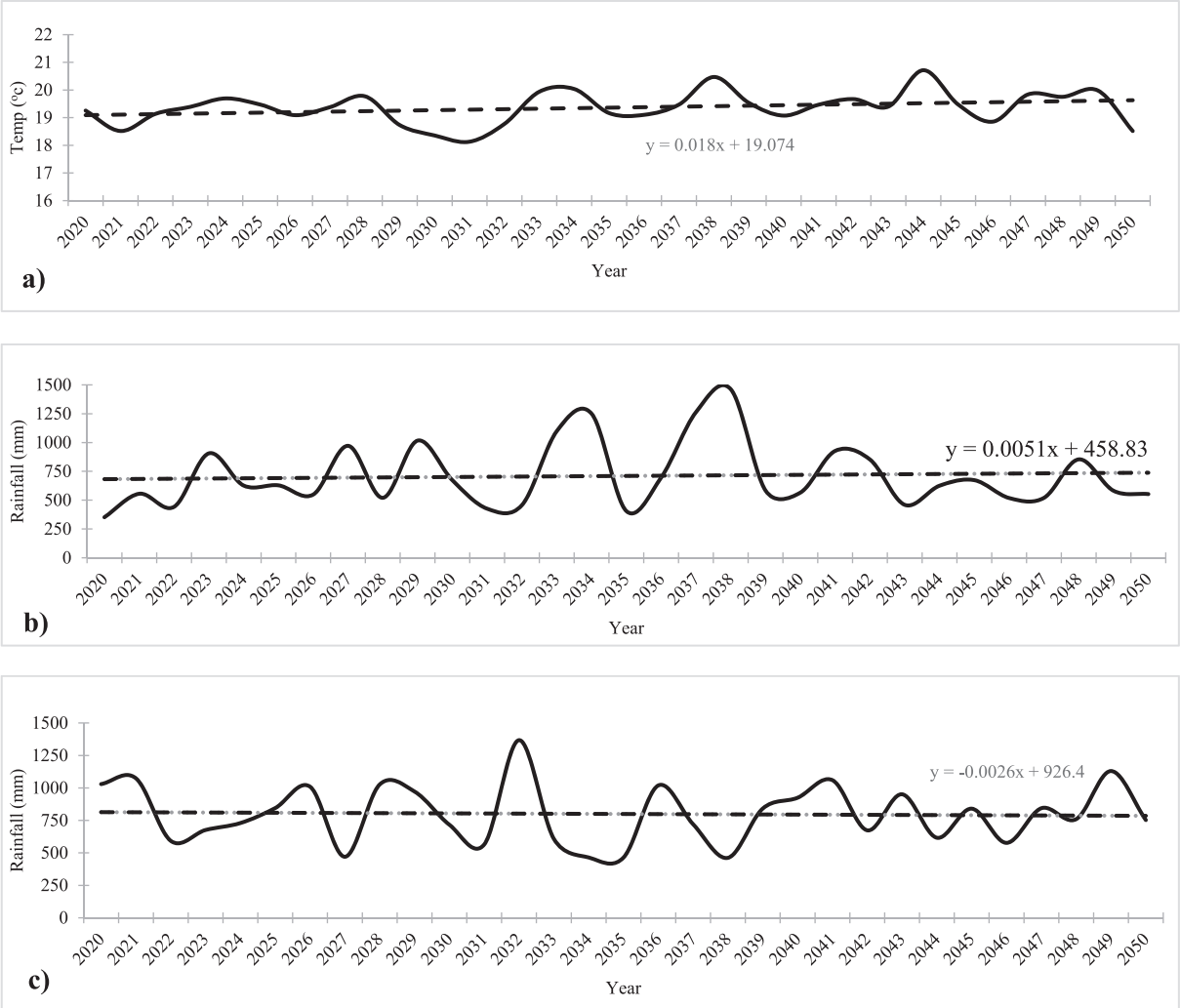

Fig. 9. Average future annual a) temperature, b) rainfall in SSP 2.45 scenario and c) rainfall in SSP 5.85 scenario.

Table 2
Average annual change in rainfall and flow under the SSP2.45 and SSP 5.85 scenarios.

mean annual change (%) in rainfall	mean annual change (%) in rainfall	mean annual change (%) in flow)
2022–2030		
SSP2.45	0.05%	−15.35
SSP5.85	0.11%	−24.93
2031–2050		
SSP2.45	1.54%	−9.27
SSP5.85	−0.01%	−14.37

increase in PET and a decrease in rainfall and flow in the future, despite the overall increasing trend in average annual temperature in the study area.

4.6. Discussions

The direct use of Global Climate Models (GCMs) for climate change forecasts at the local level is unsuitable. As seen in Fig. 4, GCM projections for Tmax were higher and Tmin was lower than observed values. However, after bias correction, these values exhibit closer alignment, yielding more plausible results. A similar challenge is observed in rainfall projections, making bias correction a crucial step to align GCM rainfall data with observed values. The model evaluation parameters, specifically R^2 (greater than 0.8) and NSE (greater than 0.7) for both monthly and daily calibration and validation in two hydrological stations, indicate that the SWAT model, coupled with SWAT-CUP, is a suitable choice for future climate change impact analysis on water availability. These values meet the acceptable criteria in hydrological modeling (R^2 greater than 0.6 and NSE greater than 0.5). Projected temperature changes show an increase from January to June and a decrease during the monsoon period (June to September). The extent of temperature change depends on the SSP scenarios. Potential changes include an increase of Tmax by up to 5.72 °C and a decrease of Tmin by up to 2.91 °C. However, in annual analysis, there is an overall increasing trend in temperature with a rate of 0.018 °C per year (Fig. 9a). Conversely, the average annual rainfall trend suggests a decrease. Under the SSP 2.45 scenario, annual rainfall would experience a slight increase of 0.0051 mm/year, while the SSP 5.85 scenario predicts a decrease of 0.0026 mm/year. In terms of average monthly rainfall analysis, a rise of 0.11% is projected for the near future, but a decline of 0.01% is anticipated under the SSP 2.45 scenario. Flow in the study area is expected to decrease by up to 15.35% under SSP 2.45 and 24.93% under SSP 5.85. The analysis of rainfall and flow patterns, as depicted in Fig. 10, suggests a potential shift in the regular rainfall during the monsoon season. Other studies in Nepalese river basins have found a similar trend in Tamor, Bagmati, Indrawati, Kaligandaki, Karnali, Bheri, and Koshi (Bharati et al., 2014; Bharati et al., 2019; Bhatta et al., 2019; V. Dahal et al., 2016; Dhami et al., 2018; Maharjan et al., 2021; Palazzoli et al., 2015). Similarly, in a research utilizing the SWAT model, (Zhou et al., 2017) discovered that the annual runoff of the Yinma River Basin (China) in the future (2021–2050) will rise by 88% for RCP 4.5 and 48% for RCP 8.5 compared to the baseline period (1981–2010). Phi Hoang et al. (2016) discovered that the ensemble flow owing to climate change increases yearly river flows in the Mekong River by +5 to +16%.

The ensemble of Global Climate Models (GCMs) estimated water availability such as surface runoff would rise between 30% and 53% in the upper region sub-basins and drop between 38% and 49% in the middle and downstream sub-basins of the study area (Fig. 11c). In the 2031–2050 timeframe, the SSP 5.85 scenario showed the most significant increase in annual surface runoff (53%), while the SSP 2.45 scenario exhibited the most substantial decline (−49%) in the upstream sub-basins. In comparison to the baseline average annual rainfall, the findings indicated a decreasing trend in rainfall for the majority of the research area's sub-basins. The projected rainfall for the SSP 2.45 and SSP 5.85 scenarios exhibited a similar pattern in the future. While the upper regions were expected to experience an increase in rainfall between 17.67% and 20.84%, the middle and downstream sub-basins were predicted the reduction in rainfall between −20.84% and − 36.34%. Fig. 11c displayed an upward trend in river flow in the upper area of the river basin (Himalayan region) but a declining trend in the western region (Indrawati and Melamchi tributaries).

5. Conclusions

In this study, we conducted an analysis of the impact of climate change on temperature, rainfall, and streamflow in the SRB. We utilized top-performing GCMs, namely MIROC6 and NorESM, under the SSP 2.45 and SSP 5.85 scenarios for the time periods of 2022–2030 and 2031–2050 to project future climate changes in the basin. Tmax (highest temperature) and Tmin (lowest temperature) were projected using MIROC6 and the Statistical Downscaling Method, while NorESM provided information on future rainfall. The calibrated SWAT model was employed to determine expected streamflow using these projections as inputs. We then used the aforementioned GCMs and scenarios, in conjunction with baseline data, to examine and compare the effects of climate change on streamflow regimes, rainfall patterns, and actual evapotranspiration in each sub-basin. The key findings of this study can be summarized as follows:

- The SWAT model performed satisfactorily during daily calibration, particularly in anticipating low flow. Evaluation indices (NSE and R^2) above 0.7 for both calibration and validation indicated the model's satisfactory performance at the daily timescale. Despite data limitations, the calibrated model provided accurate estimates of future streamflow in the SRB, faithfully reflecting the basin's hydrological processes.

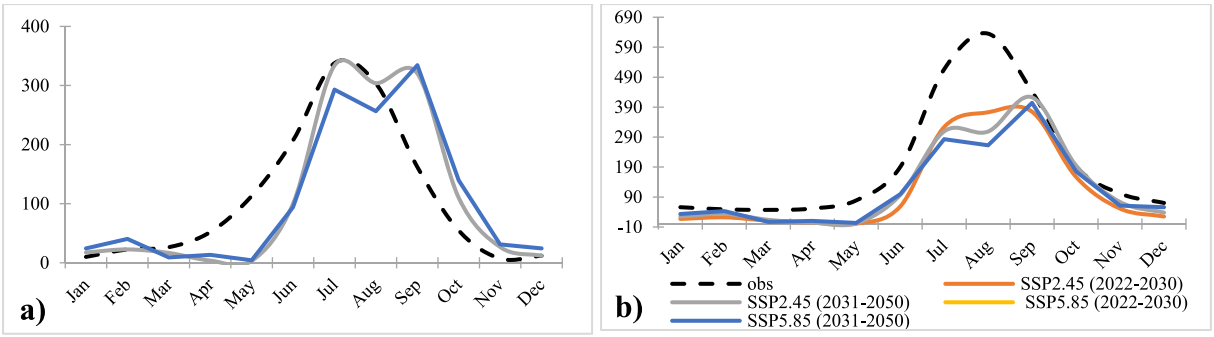

Fig. 10. Mean monthly a) rainfall and b) flow at two different scenarios in two different future time scale.

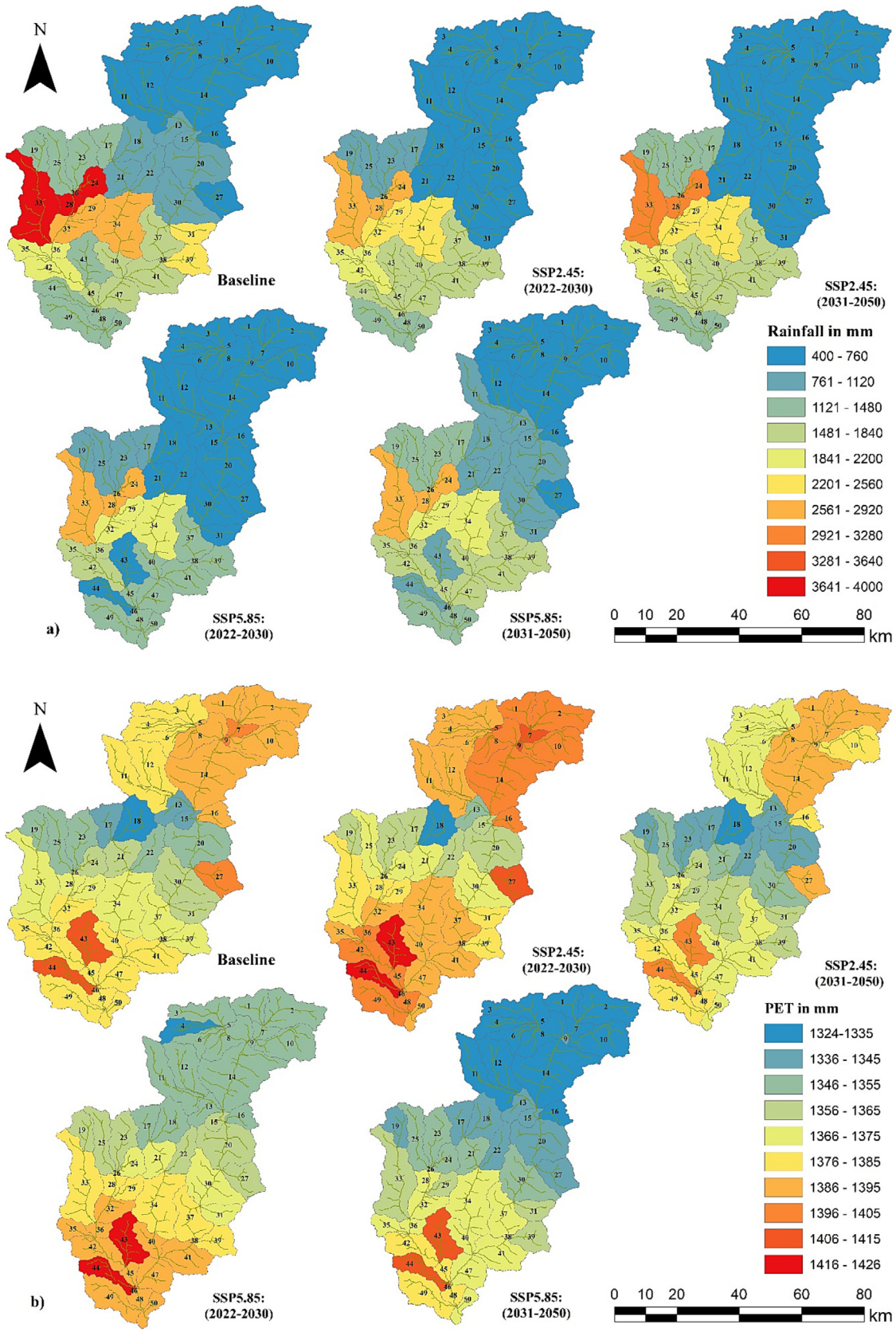

Fig. 11. Sub-basin level average annual a) rainfall, b) actual evapotranspiration and c) flow out in two scenarios at two future time with respect to baseline.

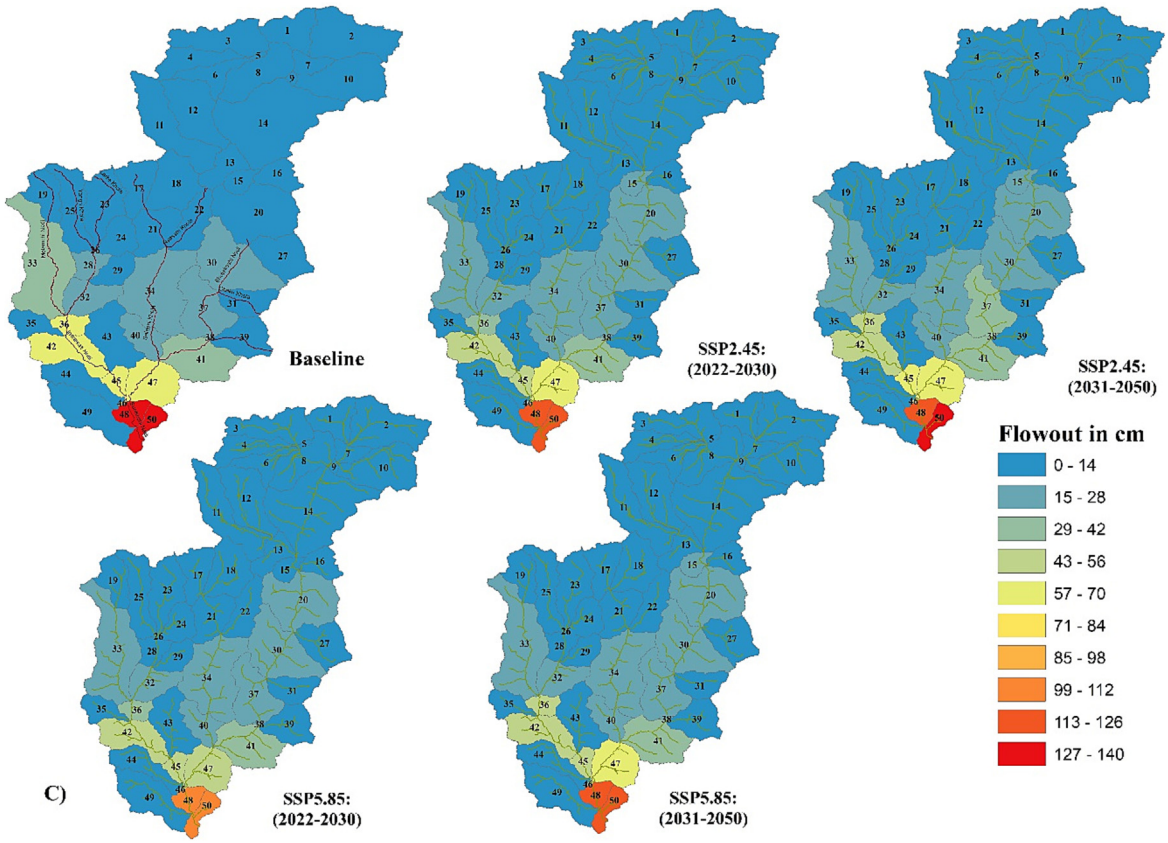

Fig 11. *Continued*

- Long-term forecasts indicated a general increase in temperatures (Tmax and Tmin) by the middle of the century. The period from January to June experienced the most significant temperature rise, followed by a slight drop from June to September during the monsoon season and modest increases from October to December. Average annual temperatures displayed an upward trend.
- Moreover, downscaled data revealed an increase in rainfall for future periods. The higher regions of the basin exhibited a maximum rise of 17.67% under the SSP 2.45 scenario and a maximum increase of 21.79% under the SSP 5.85 scenario. Conversely, downstream regions of the SRB showed decreased rainfall, ranging from −36.34% in SSP 2.45 scenarios to −20.84% in SSP 5.85 scenarios. Streamflow estimates under the SSP 2.45 scenario indicated an increase ranging from 23% to 53% and a reduction from −38% to −40%. Meanwhile, the SSP 5.85 scenario suggested an increase ranging from 14% to 27% in the near future (NF) and 36% to 54% in the mid-future (MF), with a decrease ranging from −17% to −33% in NF and − 14% to −26% in MF. Remarkably, these forecasts depicted increased streamflow in the Himalayan regions but decreased flow in the middle and lower regions, known for their agricultural practices and wooded areas with soils rich in humic and chromic CAMBISOLS.

Rainfall projections indicated an increase between 7.67% and 21.79% in the upper regions of the SRB, accompanied by reductions ranging from −20.84% to −36.34% in the lower and middle regions under different scenarios and time periods. These rainfall and PET changes aligned with the streamflow findings. The maximum anticipated increase in PET was 0.93% in the future. Consequently, projected water availability in SRB may fluctuate due to the impacts of climate change, underscoring the need for further research on how climate change will affect water resources in the basin.

CRediT authorship contribution statement

Raghu Nath Prajapati: Conceptualization, Data curation, Formal analysis, Methodology, Resources, Software, Visualization, Writing – original draft, Writing – review & editing. **Nurazim Ibrahim:** Supervision. **Bhesh Raj Thapa:** Supervision.

Declaration of Competing Interest

The authors declare no conflicts of interest.

Acknowledgements

The authors would like to thank the Department of Hydrology and Meteorology (DHM), Nepal for providing hydro-meteorological and climate data. Dipendra Gautam and Koshish Raj Maharajan are also acknowledged for their supports in errors correction and SWAT model development respectively. The authors would also like to express sincere gratitude to the anonymous reviewers for their invaluable feedback and constructive comments, which significantly enhanced the quality and rigor of this manuscript. Their expertise and thoughtful suggestions greatly contributed to the refinement of our work. Also, the dedicated editorial team are extended appreciation for their guidance and support throughout the publication process.

References

Abbaspour, K.C., Vaghefi, S.A., Yang, H., Srinivasan, R., 2019. Global soil, land use, evapotranspiration, historical and future weather databases for SWAT applications. Scientific Data 6 (1), 1–11. https://doi.org/10.1038/s41597-019-0282-4.

Zhou, Y., Xu, Y.J., Xiao, W., Wang, J., Huang, Y., Yang, H., 2017. Climate change impacts on flow and suspended sediment yield in headwaters of high-latitude regions-A case

study in China's far Northeast. Water (Switzerland) 9 (12). https://doi.org/10.3390/w9120966.
Adachi, S.A., Tomita, H., 2020. Methodology of the constraint condition in dynamical downscaling for regional climate evaluation: a review. J. Geophys. Res. Atmos. 125 (11). https://doi.org/10.1029/2019JD032166.
Agarwal, A., Babel, M.S., Maskey, S., 2015. Estimating the Impacts and Uncertainty of Climate Change on the Hydrology and Water Resources of the Koshi River Basin. Springer International Publishing Switzerland, pp. 105–126. https://doi.org/10.1007/978-3-319-10467-6.
Almazroui, M., Saeed, S., Saeed, F., Islam, M.N., Ismail, M., 2020. Projections of precipitation and temperature over the south Asian countries in CMIP6. Earth Syst. Environ. 4 (2), 297–320. https://doi.org/10.1007/s41748-020-00157-7.
Bajracharya, A.R., Bajracharya, S.R., Shrestha, A.B., Maharjan, S.B., 2018. Climate change impact assessment on the hydrological regime of the Kaligandaki Basin, Nepal. Sci. Total Environ. 625, 837–848. https://doi.org/10.1016/j.scitotenv.2017.12.332.
Basheer, A.K., Lu, H., Omer, A., Ali, A.B., Abdelgader, A.M.S., 2016. Impacts of climate change under CMIP5 RCP scenarios on the streamflow in the Dinder River and ecosystem habitats in Dinder National Park, Sudan. Hydrol. Earth Syst. Sci. 20 (4), 1331–1353. https://doi.org/10.5194/hess-20-1331-2016.
Bharati, L., Gurung, P., Jayakody, P., Smakhtin, V., Bhattarai, U., 2014. The projected impact of climate change on water availability and development in the Koshi Basin, Nepal. Mt. Res. Dev. 34 (2). https://doi.org/10.1659/MRD-JOURNAL-D-13-00096.1.
Bharati, L., Bhattarai, U., Khadka, A., Gurung, P., Neumann, L.E., Penton, D.J., Dhaubanjar, S., Nepal, S., 2019. From the mountains to the plains: impact of climate change on water resources in the Koshi River basin. IWMI Working Papers. 187. https://doi.org/10.5337/2019.205.
Bhatta, B., Shrestha, S., Shrestha, P.K., Talchabhadel, R., 2019. Evaluation and application of a SWAT model to assess the climate change impact on the hydrology of the Himalayan River Basin. Catena 181, 104082. https://doi.org/10.1016/j.catena.2019.104082.
Colette, A., Vautard, R., Vrac, M., 2012. Regional climate downscaling with prior statistical correction of the global climate forcing. Geophys. Res. Lett. 39 (13), 1–5. https://doi.org/10.1029/2012GL052258.
Dahal, P., Shrestha, M.L., Panthi, J., Pradhananga, D., 2020. Modeling the future impacts of climate change on water availability in the Karnali River basin of Nepal Himalaya. Environ. Res. 185, 1–25. https://doi.org/10.1016/j.envres.2020.109430.
Dahal, V., Shakya, N.M., Bhattarai, R., 2016. Estimating the impact of climate change on water availability in Bagmati Basin, Nepal. Environ. Proc. 3 (1), 1–17. https://doi.org/10.1007/s40710-016-0127-5.
Dai, A., Rasmussen, R.M., Ikeda, K., Liu, C., 2020. A new approach to construct representative future forcing data for dynamic downscaling. Clim. Dyn. 55 (1–2), 315–323. https://doi.org/10.1007/s00382-017-3708-8.
Dhami, B., Himanshu, S.K., Pandey, A., Gautam, A.K., 2018. Evaluation of the SWAT model for water balance study of a mountainous snowfed river basin of Nepal. Environmental Earth Sciences 77 (1), 1–20. https://doi.org/10.1007/s12665-017-7210-8.
Faramarzi, M., Abbaspour, K.C., Adamowicz, W.L.V., Lu, W., Fennell, J., Zehnder, A.J.B., Goss, G.G., 2017. Uncertainty based assessment of dynamic freshwater scarcity in semi-arid watersheds of Alberta, Canada. J. Hydrol.: Reg. Stud. 9, 48–68. https://doi.org/10.1016/j.ejrh.2016.11.003.
GIORGI, F., GAO, X.J., 2018. Regional earth system modeling: review and future directions. Atmos. Oceanic Sci. Lett. 11 (2), 189–197. https://doi.org/10.1080/16742834.2018.1452520.
Gosain, A.K., Rao, S., Basuray, D., 2006. Climate change impact assessment on hydrology of Indian river basins. Curr. Sci. 90 (3), 346–353.
Gurung, P., Bharati, L., Karki, S., 2013. Application of SWAT Model to assess the climate change impact on water balance over the cereal crops in the West Seti River Basin. 15 (January), 7933.
Imada, Y., Watanabe, M., Kawase, H., Shiogama, H., Arai, M., 2019. The July 2018 high temperature event in Japan could not have happened without human-induced global warming. Scientific Online Lett. Atmos. 15 (A), 8–12. https://doi.org/10.2151/sola.15A-002.
IPCC, 2023. AR6 Synthesis Report: Climate Change 2023. https://www.ipcc.ch/report/sixth-assessment-report-cycle/.
Kumar, D., Bhattacharjya, R.K., 2020. Evaluating two GIS-based semi-distributed hydrological models in the Bhagirathi-Alkhnanda River catchment in India. Water Policy 22 (6), 991–1014. https://doi.org/10.2166/wp.2020.159.
Maharjan, M., Aryal, A., Talchabhadel, R., Thapa, B.R., 2021. Impact of climate change on the streamflow modulated by changes in precipitation and temperature in the north latitude watershed of Nepal. Hydrology 8 (3). https://doi.org/10.3390/hydrology8030117.
Maraun, D., 2013. Bias correction, quantile mapping, and downscaling: revisiting the inflation issue. J. Clim. 26 (6), 2137–2143. https://doi.org/10.1175/JCLI-D-12-00821.1.
Marchi, M., Castellanos-Acuña, D., Hamann, A., Wang, T., Ray, D., Menzel, A., 2020. ClimateEU, scale-free climate normals, historical time series, and future projections for Europe. Scientific Data 7 (1), 1–9. https://doi.org/10.1038/s41597-020-00763-0.
Maskey, S., Uhlenbrook, S., Ojha, S., 2011. An analysis of snow cover changes in the Himalayan region using MODIS snow products and in-situ temperature data. Clim. Chang. 108 (1), 391–400. https://doi.org/10.1007/s10584-011-0181-y.
Mishra, Y., Nakamura, T., Babel, M.S., Ninsawat, S., Ochi, S., 2018. Impact of climate change on water resources of the Bheri River basin, Nepal. Water (Switzerland) 10 (2), 1–21. https://doi.org/10.3390/w10020220.
Mishra, Y., Babel, M.S., Nakamura, T., Mishra, B., 2021. Impacts of climate change on irrigation water management in the babai river basin, Nepal. Hydrology 8 (85), 1–20. https://doi.org/10.3390/hydrology8020085.
Miyamoto, Y., Kajikawa, Y., Yoshida, R., Yamaura, T., Yashiro, H., Tomita, H., 2013. Deep moist atmospheric convection in a subkilometer global simulation. Geophys. Res. Lett. 40 (18), 4922–4926. https://doi.org/10.1002/grl.50944.
Moriasi, D.N., Arnold, J.G., Van Liew, M.W., R.L., B, Harmel, R.D., Veith, T.L., 2007. Model evaluation guidelines for systematic quantification of accuracy in watershed simulation. Am. Soc. Agricult. Biol. Eng. ISSN 50 (3), 885–900.
Navarro-Racines, C., Tarapues, J., Thornton, P., Jarvis, A., Ramirez-Villegas, J., 2020. High-resolution and bias-corrected CMIP5 projections for climate change impact assessments. Scientific Data 7 (1), 1–14. https://doi.org/10.1038/s41597-019-0343-8.
Palazzoli, I., Maskey, S., Uhlenbrook, S., Nana, E., Bocchiola, D., 2015. Impact of prospective climate change on water resources and crop yields in the Indrawati basin, Nepal. Agric. Syst. 133, 143–157. https://doi.org/10.1016/J.AGSY.2014.10.016.
Pandey, V.P., Dhaubanjar, S., Bharati, L., Thapa, B.R., 2019. Hydrological response of Chamelia watershed in Mahakali Basin to climate change. Sci. Total Environ. 650, 365–383. https://doi.org/10.1016/j.scitotenv.2018.09.053.
Pandey, V.P., Dhaubanjar, S., Bharati, L., Thapa, B.R., 2020a. Spatio-temporal distribution of water availability in Karnali-Mohana Basin, Western Nepal: climate change impact assessment (part-B). J. Hydrol.: Reg. Stud. 29 (May), 100691. https://doi.org/10.1016/j.ejrh.2020.100691.
Pandey, V.P., Shrestha, D., Adhikari, M., Shakya, S., 2020b. Streamflow alterations, attributions, and implications in extended East Rapti watershed, Central-Southern Nepal. Sustainability (Switzerland) 12 (9). https://doi.org/10.3390/su12093829.
Pang, J., Zhang, H., Xu, Q., Wang, Y., Wang, Y., Zhang, O., Hao, J., 2020. Hydrological evaluation of open-access precipitation data using SWAT at multiple temporal and spatial scales. Hydrol. Earth Syst. Sci. 24 (7), 3603–3626. https://doi.org/10.5194/hess-24-3603-2020.
Phi Hoang, L., Lauri, H., Kummu, M., Koponen, J., Vliet, M.T.H.V., Supit, I., Leemans, R., Kabat, P., Ludwig, F., 2016. Mekong River flow and hydrological extremes under climate change. Hydrology and Earth System Sciences 20 (7), 3027–3041. https://doi.org/10.5194/hess-20-3027-2016.
Prein, A.F., Rasmussen, R.M., Ikeda, K., Liu, C., Clark, M.P., Holland, G.J., 2017. The future intensification of hourly precipitation extremes. Nat. Clim. Chang. 7 (1), 48–52. https://doi.org/10.1038/nclimate3168.
Richter, I., Tokinaga, H., 2020. An overview of the performance of CMIP6 models in the tropical Atlantic: mean state, variability, and remote impacts. Clim. Dyn. 55 (9–10), 2579–2601. https://doi.org/10.1007/s00382-020-05409-w.
Rocheta, E., Evans, J.P., Sharma, A., 2017. Can Bias correction of regional climate model lateral boundary conditions improve low-frequency rainfall variability? J. Clim. 30 (24), 9785–9806. https://doi.org/10.1175/JCLI-D-16-0654.1.
Sato, T., Kimura, F., Kitoh, A., 2007. Projection of global warming onto regional precipitation over Mongolia using a regional climate model. J. Hydrol. 333 (1), 144–154. https://doi.org/10.1016/j.jhydrol.2006.07.023.
Satoh, M., Stevens, B., Judt, F., Khairoutdinov, M., Lin, S.J., Putman, W.M., Düben, P., 2019. Global cloud-resolving models. Curr. Clim. Change Reports 5 (3), 172–184. https://doi.org/10.1007/s40641-019-00131-0.
Schuol, J., Abbaspour, K.C., Srinivasan, R., Yang, H., 2008. Estimation of freshwater availability in the west African sub-continent using the SWAT hydrologic model. J. Hydrol. 352 (1–2), 30–49. https://doi.org/10.1016/j.jhydrol.2007.12.025.
Shrestha, M., Acharya, S.C., Shrestha, P.K., 2017. Bias correction of climate models for hydrological modelling – are simple methods still useful? Meteorol. Appl. 24 (3), 531–539. https://doi.org/10.1002/met.1655.
Singh, L., Saravanan, S., 2020. Simulation of monthly streamflow using the SWAT model of the Ib River watershed, India. HydroResearch 3, 95–105. https://doi.org/10.1016/j.hydres.2020.09.001.
Stocker, T.F., Qin, D., Plattner, G.K., Tignor, M.M.B., Allen, S.K., Boschung, J., Nauels, A., Xia, Y., Bex, V., Midgley, P.M., 2013. Climate change 2013 the physical science basis: working group I contribution to the fifth assessment report of the intergovernmental panel on climate change. IPCC, 1–1535 https://doi.org/10.1017/CBO9781107415324 9781107057.
Tan, M.L., Ficklin, D.L., Ibrahim, A.L., Yusop, Z., 2014. Impacts and uncertainties of climate change on streamflow of the Johor River basin, Malaysia using a cmip5 general circulation model ensemble. J. Water Clim. Change 5 (4), 676–695. https://doi.org/10.2166/wcc.2014.020.
Tan, M.L., Ibrahim, A.L., Yusop, Z., Chua, V.P., Chan, N.W., 2017. Climate change impacts under CMIP5 RCP scenarios on water resources of the Kelantan River basin, Malaysia. Atmos. Res. 189, 1–10. https://doi.org/10.1016/j.atmosres.2017.01.008.
Teutschbein, C., Seibert, J., 2012. Bias correction of regional climate model simulations for hydrological climate-change impact studies: review and evaluation of different methods. J. Hydrol. 456–457, 12–29. https://doi.org/10.1016/j.jhydrol.2012.05.052.
Trenberth, K.E., 2011. Changes in precipitation with climate change. Clim. Res. 47 (1–2), 123–138. https://doi.org/10.3354/cr00953.
Uddin, K., Shrestha, H.L., Murthy, M.S.R., Bajracharya, B., Shrestha, B., Gilani, H., Pradhan, S., Dangol, B., 2015. Development of 2010 national land cover database for the Nepal. J. Environ. Manag. 148, 82–90. https://doi.org/10.1016/j.jenvman.2014.07.047.
Wang, Y., Leung, L.R., Lee, D., Wang, W., Ding, Y., 2004. Rcm_Review03. J. Meteorol. Soc. Jpn. 82 (6), 1–30 papers2://publication/uuid/56A6022E-970F-40C8-8E96-F624F1D6AA1A.
Xu, Z., Yang, Z., 2015. A new dynamical downscaling approach with GCM bias corrections and spectral nudging. J. Geophys. Res. Atmos. 10 (1002), 3063–3084. https://doi.org/10.1038/175238c0.
Xu, Z., Han, Y., Tam, C.Y., Yang, Z.L., Fu, C., 2021. Bias-corrected CMIP6 global dataset for dynamical downscaling of the historical and future climate (1979–2100). Scientific Data 8 (1), 1–11. https://doi.org/10.1038/s41597-021-01079-3.